Citrate-Induced Nanocubes: A Re-Examination of the Role of Citrate as a Shape-Directing Capping Agent for Ag-Based Nanostructures

*Maryam Hajfathalian, Kyle D. Gilroy, Robert A. Hughes, and Svetlana Neretina**

Seed-mediated syntheses utilizing facet-selective surface passivation provide the necessary chemical controls to direct noble metal nanostructure formation to a predetermined geometry. The foremost protocol for the synthesis of (111)-faceted Ag octahedra involves the reduction of metal ions onto pre-existing seeds in the presence of citrate and ascorbic acid. It is generally accepted that the capping of (111) facets with citrate dictates the shape while ascorbic acid acts solely as the reducing agent. Herein, a citrate-based synthesis is demonstrated in which the presence or absence of ascorbic acid is the shape-determining factor. Reactions are carried out in which Ag^+ ions are reduced onto substrate-immobilized Ag, Au, Pd, and Pt seeds. Syntheses lacking ascorbic acid, in which citrate acts as both the capping and the reducing agent, result in a robust nanocube growth mode able to withstand wide variations in the concentration of reactants, reaction rates, seed material, seed orientation and faceting, pH, and substrate material. If, however, ascorbic acid is included in these syntheses, then the growth mode reverts to one that advances the octahedral geometry. The implication of these results is that citrate, or one of its oxidation products, selectively caps (100) facets, but where this capability is compromised by ascorbic acid.

1. Introduction

Chemical additives that selectively bind to specific facets are well recognized for their ability to guide colloidal syntheses along pathways yielding near-identical nanostructures with highly geometric architectures.[1] The inclusion of these so-called capping agents into reaction schemes directed toward the formation of noble metal nanostructures has allowed for the synthetic flexibility needed to tailor physical, chemical, and optical properties.[2] Reactions performed under thermodynamic control in the absence of capping agents proceed along growth pathways which favor the formation of low surface energy structures. Face centered cubic (fcc) metals, which have a hierarchy of surface energies given by $\gamma\{110\} > \gamma\{100\} > \gamma\{111\}$, therefore, tend toward the formation of nanostructures dominated by (111) faceting. Suitably chosen capping agents can dramatically alter this hierarchy and, hence, promote alternate faceting while still maintaining thermodynamic control over the reaction.[3] The chemisorption of a capping agent onto a specific facet inhibits growth on that facet while allowing for the preferential growth on all other facets, a growth mode whose end product is a nanoparticle bound entirely by the capped facet.[3] Capping (100) facets, therefore, results in nanocubes, while (111) capping leads to the formation of octahedra. This synthetic strategy is particularly effective in

M. Hajfathalian, Dr. K. D. Gilroy,[+] Dr. R. A. Hughes, Prof. S. Neretina
College of Engineering
Temple University
Philadelphia, PA 19122, United States
E-mail: neretina@temple.edu

[+]Present address: The Wallace H. Coulter Department of Biomedical Engineering, Georgia Institute of Technology and Emory University, Atlanta, GA 30332, USA

DOI: 10.1002/smll.201600545

seed-mediated protocols utilizing monodisperse seeds with well-defined facets and is able to accommodate both homoepitaxial and heteroepitaxial depositions.[1a,1d,2,3b,4]

The shape engineering of noble metal nanostructures using facet-specific capping has proved to be extraordinarily successful. This success can, in large part, be attributed to the discovery of a wide assortment of capping agents able to promote both low-[1b,3b] and high-index facets.[1a,1c,5] While this synthetic strategy is conceptually straightforward, it is, in practice, complicated by numerous extraneous factors which narrow processing "windows" and provide obstacles when trying to determine the mechanistic role played by individual reagents. The seed crystallinity and faceting are critical in asserting control over the nanostructure shape. Twin defects, for example, can lead to a loss of shape uniformity but, when brought under synthetic control, can give rise to a unique set of nanostructure architectures.[6] While highly faceted monodisperse seeds seem well suited for shape modifications through facet selective capping, such seeds do not typically enter the reaction with pristine surfaces, but are instead coated with the stabilizing agent needed to prevent agglomeration and/or the capping agent used to obtain a faceted geometry. Reaction rates also play a decisive role in determining nanostructure shape, with slow, fast, and medium reaction kinetics all capable of giving rise to unique geometries.[3a,7] Shape can also be influenced by the reaction temperature,[8] the pH,[9] the presence of solvated ions,[7a] precursor concentrations,[7b] the lattice mismatch between the seed and depositing material,[10] and dissolved gases.[11] In fact, reagents are often added simply because they have been empirically demonstrated as effective in achieving a desired outcome. While the product of such reactions is often impressive, an understanding of the shape-control chemistry can, at times, be quite challenging.

The most straightforward facet-selective growth modes directed toward the formation of Ag-based nanostructures utilize a silver nitrate ($AgNO_3$) precursor in combination with reducing, capping, and stabilizing agents.[2] Trisodium citrate ($Na_3C_6H_5O_7$; abbreviated Na_3CA) has been widely used as a reagent in such syntheses because citrate can, depending upon the specifics of an individual reaction, act in each of these capacities or even take on multiple roles. In the self-seeding synthesis of Ag nanoparticles, where citrate acts as both the reductant and the stabilizing agent (i.e., the Turkevich method[12]), the product is generally considered unsatisfactory, yielding structures which are polydisperse and lack shape uniformity.[13] In this instance, citrate performs poorly as a shape-directing agent. This, however, is not the case for numerous seed-mediated syntheses which utilize citrate and achieve shape control.[1d,3,11a,14] In this regard, the seed-mediated synthesis which reduces Ag^+ ions with ascorbic acid (AA) in the presence of Na_3CA stands out as the foremost protocol for the synthesis of (111)-faceted Ag octahedra.[3] It is generally accepted that the growth mode is facilitated by the selective binding of citrate to the (111) facets, with AA remaining passive in terms of directing the shape. It is, however, understood that alterations to the pH can have a strong influence in determining the final nanostructure geometry.[9]

Mechanistic insights into solution-based growth modes are more readily obtained when examining syntheses with a small number of reagents.[5c,7a,15] Such syntheses allow individual aspects of the reaction to be more effectively isolated by minimizing the number of confounding factors arising from reagents working in cooperation or in competition with one another. Seed-mediated syntheses carried out on substrate-immobilized seeds[7a,16] can be particularly effective in this regard since immobilization negates the need for stabilizing agents. The seeds can, hence, enter the reaction with uncompromised surfaces which can be left as pristine or altered by a facet-specific capping agent. In this report, we explore the simplified two-reagent seed-mediated synthesis in which Ag^+ derived from an $AgNO_3$ precursor is reduced onto substrate-immobilized nanostructures (Ag, Au, Pd, or Pt) using citrate as the reductant and the capping agent. Our expectation of an octahedron-shaped reaction product, founded on the premise that citrate would cap (111) facets, proved to be inaccurate. Observed instead was a robust nanocube growth mode able to withstand wide variations in the growth parameters. The seeming contradiction between these results and the aforementioned colloidal growth mode, which sees (111)-faceted octahedra form in the three-reagent seed-mediated synthesis combining $AgNO_3$, Na_3CA, and AA, is reconciled through experiments which demonstrate that the nanocube geometry gives way to octahedral growth when AA is included in our synthesis.

2. Results

2.1. Citrate Reduction of Ag^+ onto Arrays of Substrate-Immobilized Au Seeds

In this reaction Ag^+ is reduced onto substrate-immobilized Au seeds to form Au–Ag core–shell structures (abbreviated Au@Ag) where citrate plays the dual role of the reducing and the capping agent. Au seeds with a diameter of ≈130 nm are formed in periodic arrays on (0001)-oriented sapphire using a templated assembly technique which we describe in detail elsewhere.[17] Seeds formed in this manner are predominantly [111]-oriented, but where other low index orientations are also observed.[18] The seed geometry is similar to that of a weakly faceted truncated octahedron, but where there exists a further planar truncation at the Au–substrate interface resulting from surface energy minimization considerations.[18,19] Such seeds are ideal from the standpoint of mechanistic studies in that they are ligand free prior to the synthesis and, by exposing both (111) and (100) facets to the growth solution, they allow for the Ag overgrowth of Au to be simultaneously monitored on two facets of high interest to solution-based growth modes.

In a typical synthesis, the substrate-supported Au seeds are placed into a heated aqueous solution of Na_3CA. Once sufficient time has elapsed to allow for temperature equilibration and the capping of Au facets with citrate, a second solution containing aqueous $AgNO_3$ is added. This initiates the reaction which sees Ag^+ reduced onto the Au seeds by citrate to form the core–shell geometry. It also results in

www.MaterialsViews.com

the formation of Ag nanoparticles suspended within the liquid medium which originate from a self-seeding growth mode where Ag clusters nucleate and grow. As a result, the growth solution evolves from clear to yellow over the duration of the synthesis. Such structures are polydisperse and show negligible faceting (Figure S1, Supporting Information); the inability of citrate to offer shape control to these structures is a result consistent with self-seeding colloidal growth modes which utilize citrate as both an Ag^+ reductant and a stabilizing agent.[13] These colloids can, however, be problematic in that they tend to bind to the substrate surface leaving unwanted Ag nanostructures adjacent to the structures nucleated by the Au seeds (Figure S2a, Supporting Information). Ultrasonication of the substrate in water immediately following the synthesis has proved to be effective in removing the majority of these structures while leaving the Au-seeded structures intact. Their spontaneous nucleation can also be severely inhibited by decreasing the pH of the growth solution to 4 through the addition of HNO_3 (Figure S2b, Supporting Information). Apart from ridding the substrate surface of these unwanted structures, this decreased pH has no obvious impact on the synthesis.

Figure 1a,b shows tilted-view scanning electron microscope (SEM) images of the arrayed structures formed through citrate reduction. The images are presented in a mixed mode format, which combines the secondary electron (SE) and backscattered electron (BSE) images, in order to highlight the Au@Ag core–shell geometry. An inspection of the arrayed structures reveals encapsulation of the inner Au core by a (100)-faceted Ag shell with sharp edges and corners. The vast majority of these structures exhibit the morphology shown in the insets to Figure 1b. The structure appears as a [111]-oriented cube relative to the underlying substrate, but where there exists a planar truncation at the cube–substrate interface. Both the cube orientation and faceting are consistent with our X-ray and electron diffraction data which show that [111]-oriented Au seeds form epitaxially on [0001]-oriented sapphire.[20] It should also be recognized that the substrate boundary prevents full encapsulation of the inner Au core with Ag. Such asymmetries are inevitable when carrying out seed-mediated syntheses at the liquid–substrate interface and, as such, lead to a unique set of nanostructure architectures which are inaccessible using standard colloidal synthesis routes.[7a,16] Plan view SEM images and the associated elemental mapping (Figure 1c) confirm the Au@Ag core–shell geometry. A comparison of the cube alignment relative to the underlying substrate (Figure 1d) reveals that these [111]-oriented structures epitaxially align with the substrate in one of two in-plane orientations differing by 180° (denoted by the upward and downward pointing arrows). The existence of these two equivalent heteroepitaxial relationships is typical for fcc metals formed on (0001)-oriented sapphire.[18] It occurs because neither the ABCABC… nor the reverse

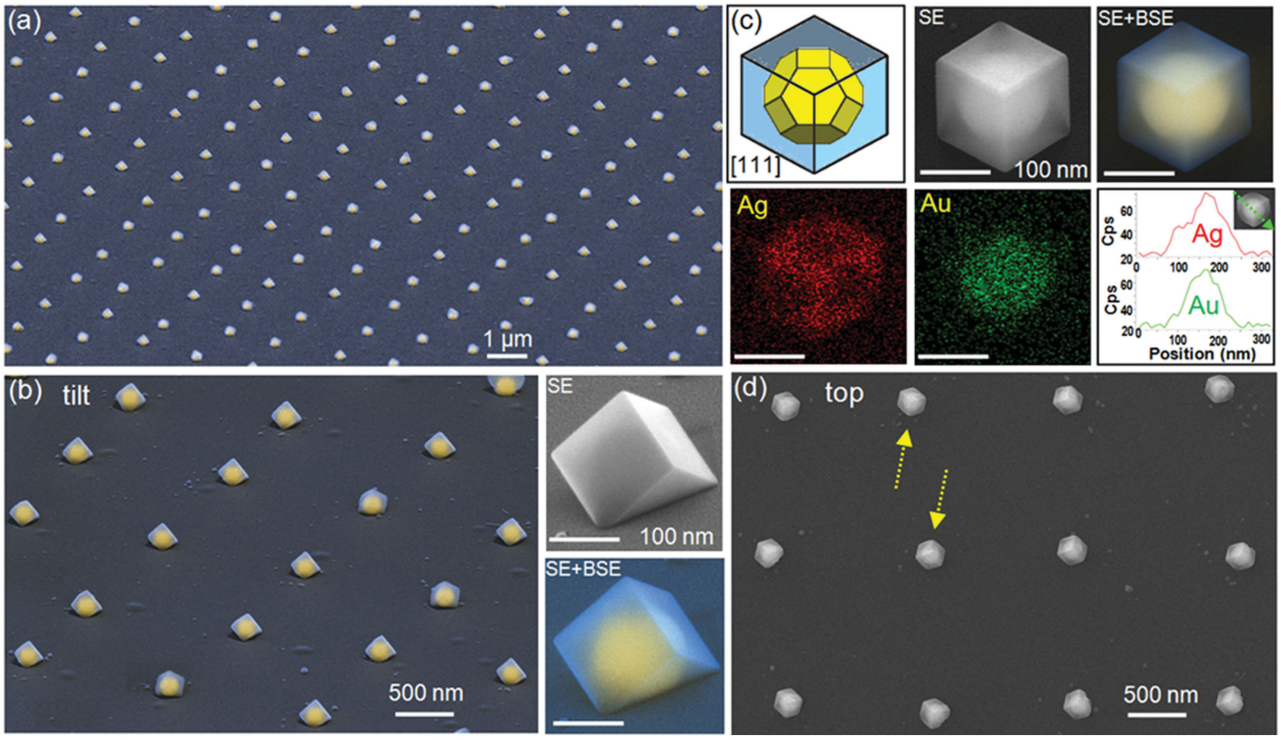

Figure 1. Morphological and elemental characterization of Au@Ag core–shell nanocube arrays formed in a seed-mediated synthesis where citrate plays the dual role of reductant and capping agent. a) Large-area 65° tilted-view SEM image of the arrayed structures. b) A higher magnification mixed mode image (SE + BSE) of the tilted array along with insets showing an individual [111]-oriented core–shell nanocube taken in both the SE and mixed mode formats. c) Schematic representation, plan view SE, and mixed mode images of a single Au@Ag core–shell nanocube and the associated elemental maps and line scans. d) Plan view SE image indicating that the nanocubes epitaxially aligned with the sapphire substrate in two orientations differing by an in-plane angle of 180° (yellow arrows).

ACBACB… stacking order along the [111]-axis of the Au seed is favored through epitaxy.[21] The synthesis of core–shell nanocubes that are epitaxially aligned with the underlying substrate is a feature unique to this work.

2.2. The Robustness of the Nanocube Growth Mode

With citrate widely accepted as a capping agent for (111) facets and the current results indicating otherwise, we began to systematically perturb the nanocube growth mode with the goal of altering it in a manner that has it reverted to the anticipated octahedral growth mode and, in the process, rationalize our unexpected results. All of these studies were carried out, not on arrayed seeds, but using Au seeds formed through the dewetting of ultrathin Au films.[22] Such seeds, while randomly positioned and showing a wide size distribution, were used because they are more easily prepared while still enabling nanocube formation (Figure S3, Supporting Information).

Initial efforts to disrupt the nanocube growth mode focused on determining the role of (i) pH, (ii) possible surface contamination of the seed, (iii) reaction kinetics, and (iv) the substrate material. The standard octahedral growth mode utilizes AA as the reducing agent and is, hence, carried out at reduced pH. In an effort to determine whether the protonation of the growth solution is capable of disrupting the nanocube growth mode, a series of syntheses were carried out where HNO_3 was added to the growth solution (**Figure 2**). It was determined that the nanocube synthesis was able to withstand a pH reduction to 3.2. Just below this value some of the (100) facets showed signs of pitting, but no (111) growth was observed. Decreasing the pH to 2.5 inhibited Ag nucleation on the Au seeds with (111) facets resulting in the least growth (denoted by yellow arrows). A further reduction of the pH to 2 further frustrated Ag nucleation. With pH effects ruled out as a means to promote an octahedral growth mode, it was deemed possible that gas molecules chemisorbed onto the seed surface or some other surface contaminant incorporated during the dewetting procedure could act as a facet-selective capping agent.[3a] The fact that the nanocube growth mode is maintained when seeds undergo ozone cleaning or when etched with dilute aqua regia argues against this possibility. In fact, these procedures seem to enhance sample quality rather than diminish it. A kinetically driven reaction which favors the formation of (100) facets instead of the thermodynamically preferred (111) facets has also been ruled out since the injection of solvated $AgNO_3$ into the growth solution by quickly pouring it in or through an injection lasting 1 h both yielded nanocubes. Further increases to the reaction kinetics resulting from a tenfold increase in the $AgNO_3$ concentration also yielded nanocubes, but where the elimination of self-nucleated Ag nanoparticles from the substrate surface becomes untenable (Figure S4, Supporting Information). We have varied concentrations widely over the course of this study for both Na_3CA (1–100 × 10^{-3} M) and $AgNO_3$ (0.2–100 × 10^{-3} M) and, while the sample quality and the degree of self-nucleated Ag nanoparticles have varied widely, nanocube formation persists showing no tendency for octahedral growth. The substrate material also had little influence upon the nanostructure faceting. In addition to the hexagonal symmetry offered by [0001]-oriented sapphire, seeds were also prepared on (100)-oriented yttria stabilized zirconia (YSZ), $(La_{0.18}Sr_{0.82})(Al_{0.59}Ta_{0.41})O_3$, and $LaAlO_3$ and (100)- and (110)-oriented $MgAl_2O_4$. An examination of the core–shell structures formed reveals that (100)-faceting occurs regardless of whether the seeds form an epitaxial relation with the substrate or not (Figure S5, Supporting Information). The only influence that the substrate seems to have on shape determination originates from the steric hindrance its planar surface exerts on the growing core–shell structure. Overall, there have been well over a hundred syntheses carried out for the Au@Ag system and, while sample quality has varied, there has never been a case where (111)-faceted octahedra emerge.

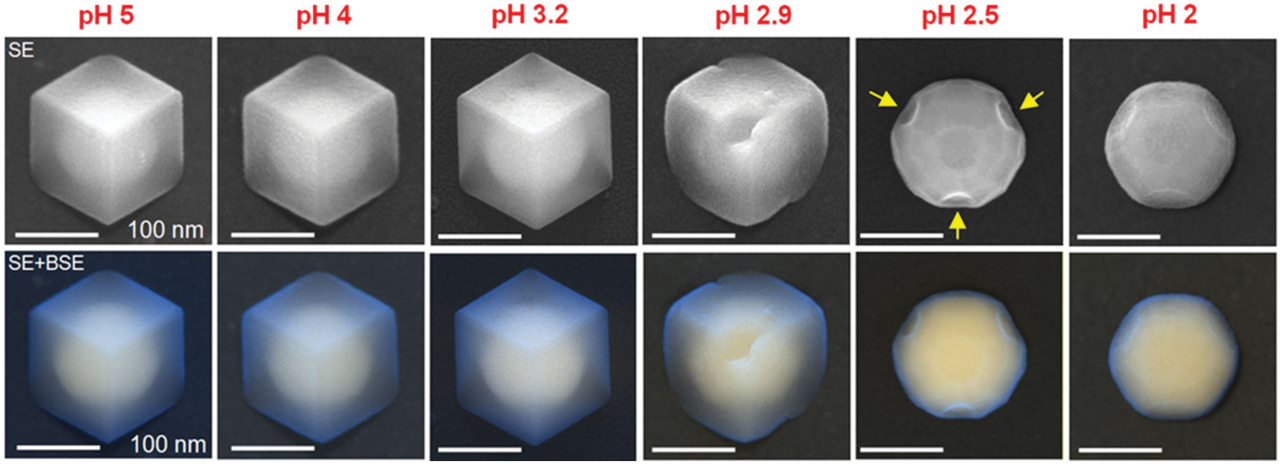

Figure 2. Plan view SEM images (top row: SE mode; bottom row: SE + BSE mode) showing the influence of reduced pH on the Au@Ag core–shell nanocube growth mode in which citrate acts as both the reductant and the capping agent. Note that, while the nanocube geometry is lost at low pH values, there is never an instance where (111) Ag faceting is observed.

www.MaterialsViews.com

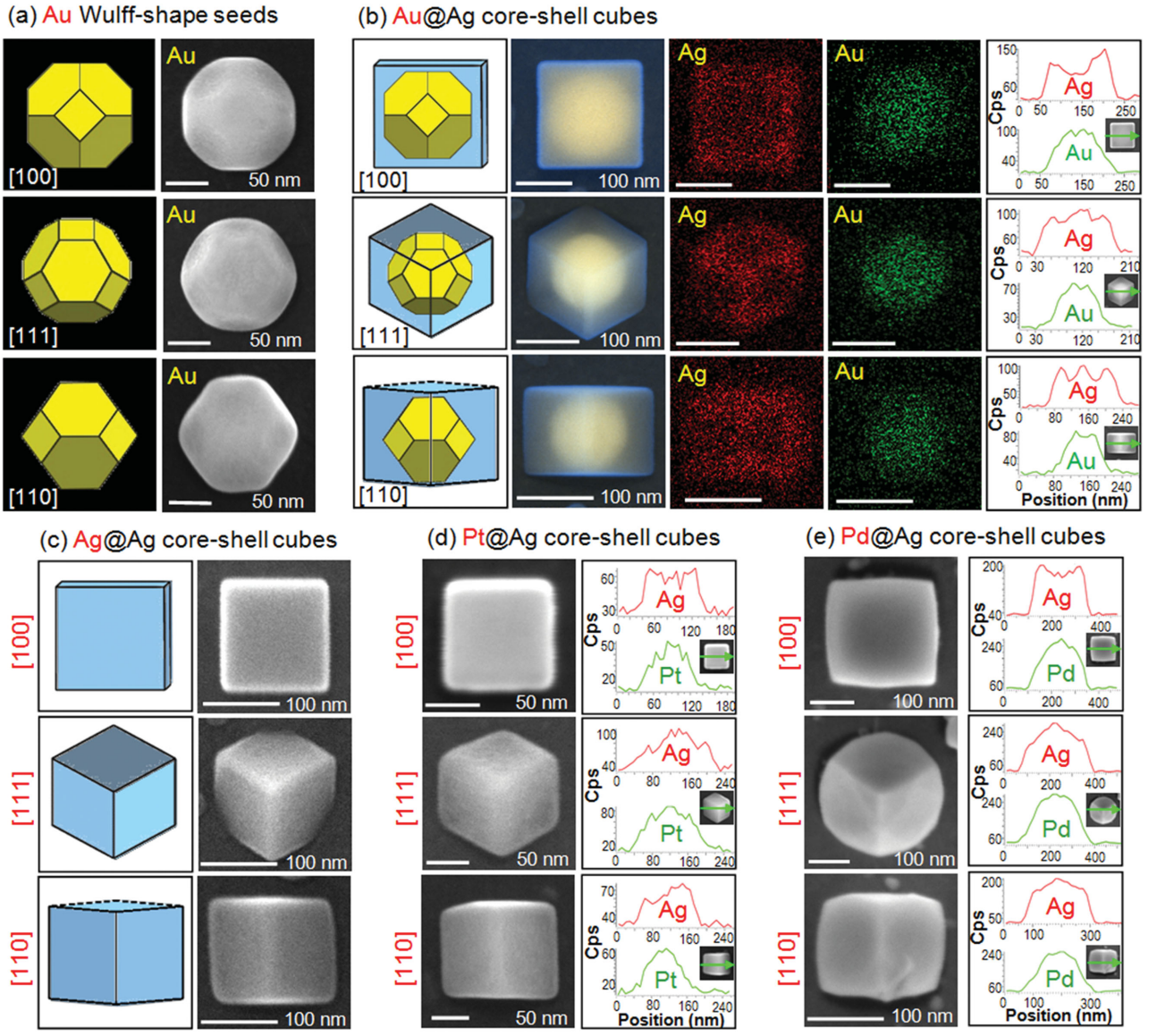

Figure 3. Schematics, plan view SEM images, and elemental mapping of a) [100]-, [111]-, and [110]-oriented Au seeds, and b) the Au@Ag nanocube structures formed when citrate is used as an Ag^+ reductant and the capping agent. Plan view SEM images and energy-dispersive X-ray spectroscopy (EDS) line scans showing that the same nanocube growth mode occurs when the synthesis utilizes seeds comprised of c) Ag, d) Pt, and e) Pd.

With the robustness of the Au@Ag nanocube growth mode established, efforts were made to determine whether the overgrowth of Ag was dependent on seed composition or its crystallographic orientation. **Figure 3** summarizes the results for seeds comprised of Au, Ag, Pt, and Pd formed through the dewetting of ultrathin films deposited on a sapphire substrate. It shows SEM images of the various seed orientations as well as compositional and morphological characterization of the structures which evolve when Ag is reduced onto [100]-, [111]-, and [110]-oriented seeds by citrate. In all cases, Ag overgrowth leads to the formation of structures with a nanocube geometry and where the core–shell structures display sharp interfaces. It is, however, noted that Pt seeds often give rise to asymmetric geometries where Ag growth seems inhibited on one side of the structure or where facets meet (Figure S6, Supporting Information).

The formation of core–shell nanocubes using Pd and Pt seeds indicates that the nanocube growth mode is able to withstand lattice mismatches between the core and shell which are as high as 4.8%. The growth mode is also able to accommodate the intricate seed geometries displayed by Pt and Pd which deviate from the equilibrium shape (i.e., the truncated octahedron) in that there are additional high-index facets.[23] The ability to form structures using Ag seeds demonstrates that this growth mode is amenable to homoepitaxial depositions capable of modifying the shape of the structure as it grows. Together, these results further attest to the robustness of the growth mode and, as a result, supports the conclusion that nanocube formation has its origins, not in some peculiarity in our synthesis, but is instead the intrinsic growth mode occurring when citrate is allowed to act as both the capping and reducing agents in this substrate-based seed-mediated synthesis.

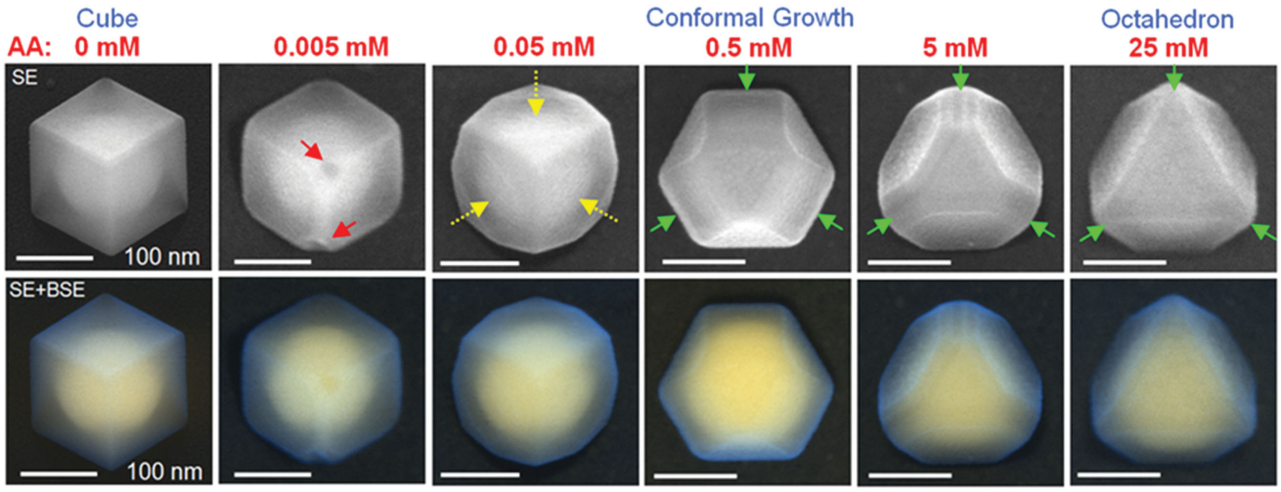

Figure 4. Plan view SEM images (top row: SE mode, bottom row: SE + BSE mode) showing the influence of increasing AA concentration on the Au@Ag core–shell nanocube growth mode. For all of these syntheses the molar concentration of Na_3CA was held constant at 10×10^{-3} M. Note that the effect of increasing AA is to transform the nanostructure geometry from a (100)-faceted cube to a (111)-faceted octahedron.

2.3. The Influence of Ascorbic Acid on the Nanocube Growth Mode

Using Au seeds, produced in the identical manner, a series of three-reagent seed-mediated syntheses were carried out in which aqueous $AgNO_3$ is injected into a solution containing 10×10^{-3} M Na_3CA where the molar concentration of AA was systematically increased from 0 to 25×10^{-3} M (**Figure 4**). At a concentration of 0.005×10^{-3} M AA, the only effect on the nanocube growth is the appearance of some imperfect corners (denoted by red arrows). At 0.05×10^{-3} M AA, the nanocube growth mode begins to break down, showing (100) facets which appear concave (yellow arrows) due to a diminishing growth rate on this facet. A further increase to 0.5×10^{-3} M leads to conformal growth with near equal growth rates on the (111) and (100) facets. As the AA concentration is increased further, the (100) facets (green arrows) decrease in size as the (111) facets progressively dominate the nanostructure geometry. The overall progression, therefore, reveals that the addition of AA to the synthesis causes the robust nanocube growth mode to give way to an octahedral geometry exhibiting the thermodynamically favored (111) facets.

3. Discussion

The results presented here as well as those recently reported by Liu et al.[16a] and Cha et al.[24] demonstrate that the seed-mediated syntheses of core–shell nanostructures can occur at the liquid–substrate interface using substrate-immobilized seeds arranged in periodic arrays. Such syntheses could advance a growing list of potential applications which take advantage of substrate-based nanostructures with the nanocube geometry.[4,25] In terms of synthesis, this work demonstrates a straightforward two-reagent reaction able to generate Ag-based core–shell nanocubes which are epitaxially aligned with the underlying substrate. Significant is that it also reveals that citrate can be used to promote the formation of (100) Ag facets. While the formation of such facets using citrate is quite unexpected, it is noted that other well-known capping agents such as poly(vinyl pyrrolidone) and cetyltrimethylammonium bromide have, under certain conditions, given rise to variable faceting.[26] We are also unaware of any colloidal synthesis which is in contradiction to our results, i.e., a seed-mediated synthesis where, in the absence of AA, (111)-faceted octahedra are formed through the reduction of Ag^+ by citrate onto Au, Ag, Pt, or Pd seeds.

On the basis of the current results, it is concluded that citrate is responsible for the selective passivation of the (100) facets and, in doing so, provides the shape-control chemistry needed to promote the nanocube geometry for this substrate-based reaction. While we concede that we provide no direct evidence for this conclusion, with only two reagents used in these reactions (i.e., Na_3CA and $AgNO_3$), it is difficult to propose an alternative explanation. While it may seem plausible that fast growth kinetics could promote the formation of structures which deviate from the equilibrium geometry, the fact that we have demonstrated that nanocube formation persists when $AgNO_3$ is slowly injected into the growth solution provides a compelling counterargument. A kinetically driven nanocube growth mode would also be contrary to our previous study[7a] which shows that fast kinetics leads to conformal growth when Ag^+ is reduced by AA onto these same surfactant-free Au seeds. Alternatively, it could be argued that the sapphire substrate is somehow responsible for the nanocube geometry, but this too seems implausible since the aforementioned study also demonstrates that surfactant-free seeds supported on a sapphire substrate can lead to the synthesis of (111)-faceted Au@Ag octahedra.

If citrate is indeed responsible for (100) capping, then there are several scenarios under which this could occur. In the first scenario, citrate would act as the selective capping agent, but where AA interferes with this capability. Citrate would, hence, promote nanocube formation only when AA is

absent or in small enough concentrations that its impact on the reaction is limited. When AA is present in quantities of significance, the capping ability of citrate is neutralized and structures supporting the more energetically favorable (111) facets prevail. This scenario would, however, predict that an analogous seed-mediated colloidal growth mode would also yield nanocubes and, if this were the case, it would require a re-examination of the role of citrate as a (111) capping agent responsible for the emergence of the octahedral geometry. Such seed-mediated syntheses are, however, not reported in the literature and, if carried out, would be in competition with Ag self-nucleation. It is noted that fundamental studies addressing citrate attachment to metal nanostructures have proven controversial,[15,27] with some supporting the preferential attachment of citrate to (111) facets and others ruling out this possibility. In a second scenario, the required (100) capping agent would be a chemical species derived from the oxidation of citrate. Such a species would, however, have to, not only cap (100) facets, but also outcompete any (111) capping by citrate over various regimes of kinetics, concentrations, and pH values. In this scenario, it would be this oxidation product which would be deactivated by small concentrations of AA and, hence, allow for the (111) capping by citrate to dominate. Possible capping agents include acetonedicarboxylate (ADC) or acetoacetate. ADC is known to form through the oxidation of citrate and has a significant impact on Au nanoparticle formation using the inverse Turkevich method.[28] Moreover, it has been demonstrated that Ag^+ ions catalyze the formation of ADC.[29] If ADC is the capping agent then the synthesis would also be complicated by the fact that the quantity present is time dependent. A third scenario is that substrate-based syntheses are fundamentally different from colloidal growth modes in a manner which has yet to be determined. Regardless of the prevailing scenario, the nanocube growth mode remains intrinsic to the use of citrate in this seed-mediated synthesis.

4. Conclusion

In summary, we have demonstrated a substrate-based nanocube growth mode occurring for the two-reagent seed-mediated synthesis in which citrate acts as both the reductant and (100) the capping agent. It has been used to fabricate periodic arrays of substrate-immobilized core–shell nanocubes where the epitaxial alignment and asymmetries imposed by the underlying substrate give rise to a unique set of nanostructures. These results were surprising in light of well-established synthetic protocols which deploy citrate as a (111) capping agent able to promote an octahedral geometry. By systematically perturbing the nanocube growth mode we have determined that it is robust to a wide range of processing conditions, but where the incorporation of AA into the synthesis sees the nanocube growth mode give way to an octahedral geometry. It is, hence, possible to reconcile this seeming contradiction through an understanding which designates citrate (or an oxidation product) as a (100) capping agent, but where this capability is compromised by an interplay between it and AA. In a broader sense, this study further demonstrates that the rich and powerful colloidal chemistry associated with noble metal nanostructures can be adapted to syntheses occurring at the liquid–substrate interface in a manner yielding both mechanistic insights and nanostructure architectures unobtainable through other means.

5. Experimental Section

Chemicals: Au, Ag, Pt, and Pd sputter targets were cut from 0.5 mm thick foils (Alfa Aesar) with purities of 99.9985%, 99.9985%, 99.99%, and 99.95%, respectively. Sb and Bi sputter targets were cut from rods with 99.999% purity (ESPI Metals). The (0001)-oriented sapphire and (100)-oriented substrates of YSZ, $MgAl_2O_4$, $(La_{0.18}Sr_{0.82})(Al_{0.59}Ta_{0.41})O_3$, and $LaAlO_3$ with dimensions of $7 \times 7 \times 0.5$ mm were cleaved from larger wafers sourced from MTI Corporation. The seed assembly processes were carried out in ultrahigh purity Ar. The solution-based syntheses utilized 99.9999% silver nitrate (Sigma Aldrich), 99% trisodium citrate dihydrate (Alfa Aesar), 99% L-ascorbic acid (Fisher Scientific), HCl (Alfa Aesar), and nitric acid (Sigma Aldrich). Deionized (DI) water with a resistivity of 18.2 MΩ cm^{-1} was used for the preparation of all aqueous solutions. Glassware was cleaned with aqua regia and thoroughly rinsed in DI water prior to use. All chemicals were used as received.

Vapor Phase Seed Assembly Processes: Substrate-immobilized seeds were prepared as either randomly positioned structures with a substantial size distribution or as periodic arrays with a narrow size distribution using vapor phase assembly techniques described in detail elsewhere.[17,22] The assembly of the randomly positioned structures was reliant on the thermal dewetting of ultrathin sputter deposited films,[22a] but where sacrificial layers of Sb or Bi were sometimes used (i.e., for Pt and Pd) to enhance the dewetting process and provide superior shape uniformity.[17] The periodic arrays of Au were prepared using a lithography-free templated assembly technique which also employed a sacrificial layer of Sb.[17] When sacrificial layers were used, the reproducibility and overall sample quality in solution-based reactions were improved when the seeds were dipped into dilute aqua regia (5×10^{-3} M, molar ratio HCl:HNO_3 is 3:1) for 5 s and then rinsed in DI water. It was suspected that this improvement stems from the dissolution of contaminants from the sacrificial layer which remained on the seed surface in small quantities. It is, however, important to note that the nanocube growth mode persists whether or not these sacrificial layers and/or aqua regia are used. All templates were assembled in a tube furnace with flowing Ar (65 sccm) where a dedicated quartz tube was used for each seed material in order to avoid cross-contamination.

Citrate-Induced Nanocube Formation: In the standard nanocube synthesis, solutions containing 3 mL of 1×10^{-3} M $AgNO_3$ and 1 mL of 10×10^{-3} M Na_3CA were preheated to 95 °C. The substrate-immobilized seeds were then placed at the bottom of the reaction vessel containing Na_3CA and allowed to equilibrate for 1 min. The reaction was then initiated by adding the $AgNO_3$ solution and allowed to proceed for 5 min. Over this time interval the color of the solution transformed from clear to yellow due to the spontaneous nucleation and growth of colloidal silver. The substrate was then removed from the reaction vessel and rinsed in DI water for 30 s while undergoing ultrasonication in order to remove

colloidal Ag adhered to the substrate surface. The sample was then removed from the water and dried in a flow of compressed air. The pH dependence shown in Figure 2 was obtained by adding varying amounts of HNO_3 to the Na_3CA solution.

Three-Reagent Syntheses Utilizing $AgNO_3$, Na_3CA, and AA: The three reagent syntheses, which gave rise to the results in Figure 4, were carried out in order to establish the influence of AA on nanocube formation. The syntheses proceeded in a manner identical to the two-reagent reaction except that varying amounts of AA (0.005 to 25×10^{-3} M) were added to the Na_3CA solution. The $AgNO_3$ was then added in a dropwise manner.

Instrumentation: All of the depositions required to form substrate-based seeds were carried out using a model 681 Gatan high-resolution ion beam coater. The seed assembly processes were carried out in a Lindberg Blue M tube furnace. SEM images, EDS cross-sections, and elemental maps were all obtained using an FEI 450 FEG ESEM. Transmission electron microscopy (TEM) measurements utilized a JEOL JEM-1400 Transmission Electron Microscope.

Supporting Information

Supporting Information is available from the Wiley Online Library or from the author.

Acknowledgements

This work was funded by a National Science Foundation award (No. DMR-1505114) to S.N. It was benefited from the facilities available through Temple University's Nano Instrumentation Center as well as the expertise of D. A. Dikin (Facility Manager). TEM measurements were carried out at Temple University's Material Research Facility (MRF) with the assistance of B. Tangeysh. K.D.G. acknowledges support received through a Temple University Graduate Fellowship. The authors also acknowledge the help received from A. Yaghoubzade in the preparation of this manuscript.

[1] a) M. L. Personick, C. A. Mirkin, *J. Am. Chem. Soc.* **2013**, *135*, 18238; b) J. Zeng, Y. Zheng, M. Rycenga, J. Tao, Z.-Y. Li, Q. Zhang, Y. Zhu, Y. Xia, *J. Am. Chem. Soc.* **2010**, *132*, 8552; c) M. R. Langille, M. L. Personick, J. Zhang, C. A. Mirkin, *J. Am. Chem. Soc.* **2012**, *134*, 14542; d) Y. Xiong, Y. Xia, *Adv. Mater.* **2007**, *19*, 3385.

[2] M. Rycenga, C. M. Cobley, J. Zeng, W. Li, C. H. Moran, Q. Zhang, D. Qin, Y. Xia, *Chem. Rev.* **2011**, *111*, 3669.

[3] a) Y. Xia, X. Xia, H.-C. Peng, *J. Am. Chem. Soc.* **2015**, *137*, 7947; b) X. Xia, J. Zeng, Q. Zhang, C. H. Moran, Y. Xia, *J. Phys. Chem. C* **2012**, *116*, 21647.

[4] J. Li, J. Liu, Y. Yang, D. Qin, *J. Am. Chem. Soc.* **2015**, *137*, 7039.

[5] a) M. L. Personick, M. R. Langille, J. Zhang, C. A. Mirkin, *Nano Lett.* **2011**, *11*, 3394; b) H.-E. Lee, K. D. Yang, S. M. Yoon, H.-Y. Ahn, Y. Y. Lee, H. Chang, D. H. Jeong, Y.-S. Lee, M. Y. Kim, K. T. Nam, *ACS Nano* **2015**, *9*, 8384; c) X. Xia, J. Zeng, B. McDearmon, Y. Zheng, Q. Li, Y. Xia, *Angew. Chem.* **2011**, *123*, 12750.

[6] a) M. L. Personick, M. R. Langille, J. Zhang, J. Wu, S. Li, C. A. Mirkin, *Small* **2013**, *9*, 1947; b) J. L. Elechiguerra, J. Reyes-Gasga, M. J. Yacaman, *J. Mater. Chem.* **2006**, *16*, 3906; c) J. Zhang, M. R. Langille, C. A. Mirkin, *J. Am. Chem. Soc.* **2010**, *132*, 12502; d) Y. Xiong, J. M. McLellan, Y. Yin, Y. Xia, *Angew. Chem.* **2007**, *119*, 804.

[7] a) K. D. Gilroy, R. A. Hughes, S. Neretina, *J. Am. Chem. Soc.* **2014**, *136*, 15337; b) C. Zhu, J. Zeng, J. Tao, M. C. Johnson, I. Schmidt-Krey, L. Blubaugh, Y. Zhu, Z. Gu, Y. Xia, *J. Am. Chem. Soc.* **2012**, *134*, 15822; c) Y. Yang, W. Wang, X. Li, W. Chen, N. Fan, C. Zou, X. Chen, X. Xu, L. Zhang, S. Huang, *Chem. Mater.* **2013**, *25*, 34.

[8] J. Zhu, F. Zhang, B.-B. Chen, J.-J. Li, J.-W. Zhao, *Mater. Sci. Eng., B* **2015**, *199*, 113.

[9] a) X. Dong, X. Ji, H. Wu, L. Zhao, J. Li, W. Yang, *J. Phys. Chem. C* **2009**, *113*, 6573; b) K. K. Caswell, C. M. Bender, C. J. Murphy, *Nano Lett.* **2003**, *3*, 667.

[10] a) F.-R. Fan, D.-Y. Liu, Y.-F. Wu, S. Duan, Z.-X. Xie, Z.-Y. Jiang, Z.-Q. Tian, *J. Am. Chem. Soc.* **2008**, *130*, 6949; b) S. E. Habas, H. Lee, V. Radmilovic, G. A. Somorjai, P. Yang, *Nat. Mater.* **2007**, *6*, 692.

[11] a) X. Wu, P. L. Redmond, H. Liu, Y. Chen, M. Steigerwald, L. Brus, *J. Am. Chem. Soc.* **2008**, *130*, 9500; b) Q. Zhang, C. Cobley, L. Au, M. McKiernan, A. Schwartz, L.-P. Wen, J. Chen, Y. Xia, *ACS Appl. Mater. Interfaces* **2009**, *1*, 2044.

[12] J. Turkevich, P. C. Stevenson, J. Hillier, *Discuss. Faraday Soc.* **1951**, *11*, 55.

[13] a) Z. S. Pillai, P. V. Kamat, *J. Phys. Chem. B* **2004**, *108*, 945; b) A. Henglein, M. Giersig, *J. Phys. Chem. B* **1999**, *103*, 9533.

[14] B. Lim, Y. Xiong, Y. Xia, *Angew. Chem.* **2007**, *119*, 9439.

[15] Q. Zhang, N. Li, J. Goebl, Z. Lu, Y. Yin, *J. Am. Chem. Soc.* **2011**, *133*, 18931.

[16] a) G. Liu, C. Zhang, J. Wu, C. A. Mirkin, *ACS Nano* **2015**, *9*, 12137; b) K. D. Gilroy, A. Sundar, P. Farzinpour, R. A. Hughes, S. Neretina, *Nano Res.* **2014**, *7*, 365; c) K. D. Gilroy, P. Farzinpour, A. Sundar, R. A. Hughes, S. Neretina, *Chem. Mater.* **2014**, *26*, 3340.

[17] P. Farzinpour, A. Sundar, K. D. Gilroy, Z. E. Eskin, R. A. Hughes, S. Neretina, *Nanoscale* **2013**, *5*, 1929.

[18] K. D. Gilroy, A. Sundar, M. Hajfathalian, A. Yaghoubzade, T. Tan, D. Sil, E. Borguet, R. A. Hughes, S. Neretina, *Nanoscale* **2015**, *7*, 6827.

[19] C. R. Henry, *Prog. Surf. Sci.* **2005**, *80*, 92.

[20] A. Sundar, P. Farzinpour, K. D. Gilroy, T. Tan, R. A. Hughes, S. Neretina, *Cryst. Growth Des.* **2013**, *13*, 3847.

[21] H. Bialas, K. Heneka, *Vacuum* **1994**, *45*, 79.

[22] a) P. Farzinpour, A. Sundar, K. D. Gilroy, Z. E. Eskin, R. A. Hughes, S. Neretina, *Nanotechnology* **2012**, *23*, 495604; b) C. V. Thompson, *Annu. Rev. Mater. Res.* **2012**, *42*, 399.

[23] A. Altberg, G. Atiya, V. Mikhelashvilli, G. Eisenstein, W. D. Kaplan, *J. Mater. Sci.* **2014**, *49*, 3917.

[24] S. K. Cha, J. H. Mun, T. Chang, S. Y. Kim, J. Y. Kim, H. M. Jin, J. Y. Lee, J. Shin, K. H. Kim, S. O. Kim, *ACS Nano* **2015**, *9*, 5536.

[25] a) P. Yang, L. Wang, Q. Wu, Z. Chen, X. Lin, *Sens. Actuators, B* **2014**, *194*, 71; b) B. Wang, L. Zhang, X. Zhou, *Spectrochim. Acta, Part A* **2014**, *121*, 63; c) L. Zhang, Y. Zhang, Y. Hu, Q. Fan, W. Yang, A. Li, S. Li, W. Huang, L. Wang, *Chem. Commun.* **2015**, *51*, 294; d) D. Sikdar, W. Cheng, M. Premaratne, *J. Appl. Phys.* **2015**, *117*, 083101; e) D. Prezgot, A. Ianoul, *J. Phys. Chem. C* **2015**, *119*, 3293; f) T. B. Hoang, G. M. Akselrod, C. Argyropoulos, J. Huang, D. R. Smith, M. H. Mikkelsen, *Nat. Commun.* **2015**, *6*, 7788; g) D. E. Gorka, J. S. Osterberg, C. A. Gwin, B. P. Colman, J. N. Meyer, E. S. Bernhardt, C. K. Gunsch, R. T. DiGulio, J. Liu, *Environ. Sci. Technol.* **2015**, *49*, 10093; h) Y. Yang, J. Liu, Z.-W. Fu, D. Qin, *J. Am. Chem. Soc.* **2014**, *136*, 8153; i) N. M. Kha, C.-H. Chen, W.-N. Su, J. Rick, B.-J. Hwang, *Phys. Chem. Chem. Phys.* **2015**, *17*, 21226.

[26] a) E. C. Cho, P. H. C. Camargo, Y. Xia, *Adv. Mater.* **2010**, *22*, 744; b) H.-Y. Ahn, H.-E. Lee, K. Jin, K. T. Nam, *J. Mater. Chem. C* **2013**, *1*, 6861.

[27] a) J.-W. Park, J. S. Shumaker-Parry, *J. Am. Chem. Soc.* **2014**, *136*, 1907; b) G. Teobaldi, F. Zerbetto, *J. Phys. Chem. C* **2007**, *111*, 13879; c) D. S. Kilin, O. V. Prezhdo, Y. Xia, *Chem. Phys. Lett.* **2008**, *458*, 113; d) R. J. Nichols, I. Burgess, K. L. Young, V. Zamlynny, J. Lipkowski, *J. Electroanal. Chem.* **2004**, *563*, 33; e) Y. Lin, G.-B. Pan, G.-J. Su, X.-H. Fang, L.-J. Wan, C.-L. Bai, *Langmuir* **2003**, *19*, 10000.

[28] a) F. Schulz, T Homolka, N. G. Bastús, V. Puntes, H. Weller, T. Vossmeyer, *Langmuir* **2014**, *30*, 10779; b) Ojea-Jiménez, N. G. Bastús, V. Puntes, *J. Phys. Chem. C* **2011**, *115*, 15752.

[29] H. Xia, S. Bai, J. Hartmann, D. Wang, *Langmuir* **2010**, *26*, 3585.

Received: February 18, 2016
Revised: April 12, 2016
Published online: May 13, 2016